

Unsteady MHD Free Convection Past an Impulsively Started Isothermal Vertical Plate with Radiation and Viscous Dissipation

Hawa Singh¹, Paras Ram² and Vikas Kumar³

Abstract: The fluctuating flow produced by magneto - hydrodynamic free convection past an impulsively started isothermal vertical plate is studied taking into account the effects of radiation and viscous dissipation. By using the similarity transformation, the governing equations are transformed into dimensionless form and then the system of nonlinear partial differential equations is solved by a perturbation technique. The considered uniform magnetic field acts perpendicular to the plate, which absorbs the fluid with a given suction velocity. A comparison is made in velocity and temperature profiles for two particular cases of real and imaginary time dependent functions. The effects of various parameters like Prandtl number, Grashof number, magnetic parameter, radiation parameter, Eckert number and Schmidt number on the velocity and temperature profiles are studied quantitatively and are shown graphically. In case of real function, the frequency of excitation ω does not have much effect over temperature and velocity profiles, respectively, whereas in case of imaginary function, it has a significant effect along the wall and transverse to the wall.

Keywords: MHD, Schmidt number, Eckert number, radiation, perturbation method, unsteady flow.

Nomenclature

u^*, v^* Velocity components in x^*, y^* direction, respectively
 y Non-dimensional distance to the surface
 \bar{u} Uniform velocity of the plate

¹ Deptt. of Mathematics, National Institute of Technology Kurukshetra, Haryana, India.
E-mail: hawasingh_nit@yahoo.com

² Deptt. of Mathematics, National Institute of Technology Kurukshetra, Haryana, India.
E-mail: parasram_nit@yahoo.co.in

³ Deptt. of Mathematics, National Institute of Technology Kurukshetra, Haryana, India.
E-mail: vksingla.nitkkr@yahoo.com

| | |
|------------|--|
| $U^*(t)$ | Dimensional free stream velocity |
| $U(t)$ | Dimensionless free stream velocity |
| V | Constant suction velocity |
| t^* | Dimensional time |
| t | Dimensionless time |
| B_0 | Magnetic induction |
| D | Mass diffusion coefficient/ chemical molecular diffusivity |
| M | Magnetic field parameter |
| g | Acceleration due to Earth's gravity |
| T^* | Dimensional temperature |
| T_w | Temperature at the wall |
| T_∞ | Free stream dimensional temperature |
| C^* | Dimensional concentration |
| C | Dimensionless concentration |
| C_w | Wall concentration |
| C_∞ | Concentration away from the wall |
| c_p | Specific heat at constant pressure |
| k_e | Mean absorption coefficient |
| k | Thermal conductivity |
| q_r | Radiative heat flux |
| R | Radiation parameter |
| Pr | Prandtl number |
| Ec | Eckert number (viscous dissipation parameter) |
| Sc | Schmidt number |
| Gr | Thermal Grashof number |
| Gm | Solutal Grashof number |

Greek Symbols

| | |
|---------------|---|
| β^* | Volumetric coefficient of concentration expansion |
| β | Coefficient of thermal expansion |
| α | Thermal diffusivity |
| θ | Dimensionless temperature |
| ρ | Fluid density |
| σ | Fluid electrical conductivity |
| σ_s | Stefan-Boltzmann constant |
| ε | Scalar constant (perturbation parameter < 1) |
| ω^* | Constant |
| ω | Frequency of oscillation ($\ll 1$) |

| | |
|----------|---|
| ν | Kinematic viscosity of the fluid at a point |
| ∞ | Ambient condition |
| * | Dimensional properties |

1 Introduction

The radiation effects are found to be more significant in the following areas of applications such as soil physics, geothermal energy extraction, chemical engineering, glass production, furnace design, space technology application, fight aerodynamics and plasma physics which operates at extremely high temperature. Also, the application of radiation heat transfer becomes highly significant in the design of pertinent equipment, viscous mechanical dissipation effects are important in geophysical flows and also in certain industrial operations and are usually characterized by Eckert number. Recently, attention has been on the effects of transversely applied magnetic field and thermal perturbation on the flow of electrically conducting viscous fluid such as plasma. Various properties associated with the interplay of magnetic fields and thermal perturbation in porous medium past vertical plate find useful applications in astrophysics, geophysical fluid dynamics and engineering.

Abd EI-Naby *et al.* (2003) presented the effects of radiation on MHD unsteady free convection flow over vertical plate with variable surface temperature. Chamkha *et al.* (2001) have studied the effects of radiation on free convection flow past a semi-infinite vertical plate with mass transfer. Das *et al.* (1994) presented the effects of mass transfer on flow past an impulsively started infinite vertical plate with constant heat flux and chemical reaction concentration of the fluid under consideration. The influence of viscous dissipation and radiation on unsteady MHD free convection flow past an infinite heated vertical plate in a porous medium with time dependent suction had been examined by Israel-Cookey *et al.* (2003). Israel-Cookey and Nwaigwe (2010) have described an electrically conducting unsteady flow and radiating fluid over a moving heated porous plate in the presence of an induced magnetic field. The effect of radiation and first order homogeneous chemical reaction with heat and mass transfer of a Newtonian, viscous, electrically conducting and heat generation/ absorption fluid on a vertical surface have been investigated by Ibrahim *et al.* (2008).

The effects of radiation on the flow past an impulsively started vertical plate in the presence of mass transfer have been investigated by Loganathan and Ganesan (2006). Subsequently, Muthucumaraswamy and Ganesan (1998, 2004) have obtained the natural convection on flow past an impulsively started vertical plate with variable surface heat flux and studied the problem of unsteady flow past an impulsively started isothermal vertical plate with mass transfer by an implicit finite dif-

ference method. Makinde (2005) studied the problem of free convection boundary layer flow with thermal radiation and mass transfer past a permeable vertical plate moves in its own plane. Radiation and mass transfer effects on two-dimensional flows past an impulsively started isothermal vertical plate have been studied by Ramachandra Prasad *et al.* (2007). Rapits and Perdakis (1999) analysed the effects of thermal radiation on free convective flow past a moving vertical plate. The effects of dissipation on an unsteady two-dimensional laminar convective boundary layer flow along a semi - infinite vertical plate with suction were studied by Ramana Murthy and Prasad (2011).

Ramana Murthy *et al.* (2010) studied the effects of thermal radiation on the natural convective heat and mass transfer of a viscous incompressible fluid flowing past an impulsively started moving vertical plate with viscous dissipation. Suneetha *et al.* (2011) analyzed radiation and mass transfer effects on MHD flow past an impulsively started vertical plate in the presence of heat source/ sink by taking into account the heat due to viscous dissipation. Takhar *et al.* (2003) employed a Runge-Kutta-Merson shooting quadrature and Rosseland diffusion algebraic radiation model to analyze the mixed radiation-convection flow in a non-Darcy porous medium, showing the temperature gradients are boosted with radiative flux. The effects of porosity on unsteady MHD free convective boundary layer flow along a semi-infinite vertical plate with time dependent suction by taking into account the effects of dissipation has been examined by Ram *et al.* (2013).

In the present study, we have discussed the unsteady MHD free convection, incompressible, electrical conducting and radiating fluctuating flow by taking into account the effects of viscous dissipation and described the comparison of velocity and temperature profiles for two particular cases of real and imaginary time dependent functions. The characteristic performance of various parameters that affects the flow entities have been discussed quantitatively and illustrated graphically. This problem, to the best of our knowledge, has not been investigated yet.

2 Mathematical formulation of the problem

An unsteady two dimensional laminar boundary layer flow of a viscous incompressible, radiating and electrically conducting fluid along a semi-infinite vertical plate with constant suction by considering the effects of viscous dissipation into account has been discussed. The x-axis is taken along the vertical plate in the upward direction and y-axis is normal to the plate. Initially, it is assumed that the plate and the fluid are of the same temperature and concentration in a stationary condition. At the time $t^* > 0$, the plate starts moving impulsively in the vertical direction with constant velocity \bar{u} against the gravitational field. It is also assumed that there is no chemical reaction between the diffusing species and the fluid. Then under the usual

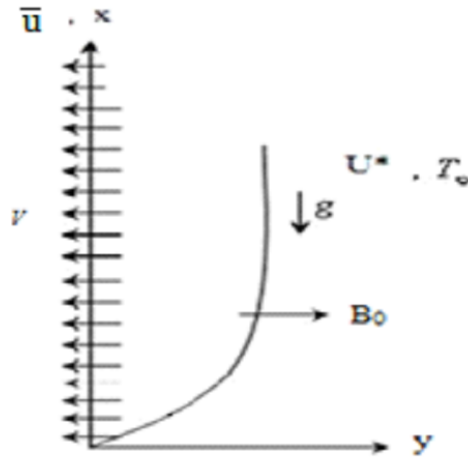


Figure a: Physical sketch of the Problem.

Boussinesq’s approximation, the unsteady flow past a vertical plate is governed by the following equations:

$$\frac{\partial v^*}{\partial y^*} = 0 \tag{1}$$

$$\frac{\partial u^*}{\partial t^*} + v^* \frac{\partial u^*}{\partial y^*} = g\beta(T^* - T_\infty) + g\beta^*(C^* - C_\infty) + v \frac{\partial^2 u^*}{\partial y^{*2}} - \sigma \frac{B_0^2 u^*}{\rho} \tag{2}$$

$$\frac{\partial T^*}{\partial t^*} + v^* \frac{\partial T^*}{\partial y^*} = \alpha \frac{\partial^2 T^*}{\partial y^{*2}} - \frac{1}{\rho c_p} \frac{\partial q_r}{\partial y^*} + \frac{v}{c_p} \left(\frac{\partial u^*}{\partial y^*} \right)^2 \tag{3}$$

$$\frac{\partial C^*}{\partial t^*} + v^* \frac{\partial C^*}{\partial y^*} = D \frac{\partial^2 C^*}{\partial y^{*2}} \tag{4}$$

The boundary conditions for the velocity, temperature and concentration fields are:

$$\left. \begin{aligned} t^* \leq 0 : u^* = 0, v^* = 0, T^* = T_\infty, C^* = C_\infty \\ t^* > 0 : u^* = \bar{u}, v^* = -V, T^* = T_w, C^* = C_w \text{ at } y^* = 0 \\ u^* = U^*(t^*), T^* = T_\infty, C^* = C_\infty \text{ at } x^* = 0 \\ u^* \rightarrow U^*(t^*), T^* \rightarrow T_\infty, C^* \rightarrow C_\infty \text{ as } y^* \rightarrow \infty \end{aligned} \right\} \tag{5}$$

We assumed that thermal radiation in the form of a unidirectional flux in the y-direction i.e., q_r (transverse to the vertical surface). By using the Rosseland approximation [Brewster (1992)], the radiative heat flux q_r is given by:

$$q_r = -\frac{4\sigma_s}{3k_e} \frac{\partial T^{*4}}{\partial y^*} \tag{6}$$

If the temperature difference $T^* - T_\infty$ within the flow is sufficiently small, the Taylor series for T^{*4} with neglect of the higher order terms is given by a linear temperature function:

$$T^{*4} \cong 4T_\infty^3 T^* - 3T_\infty^4 \tag{7}$$

By using equations (6) and (7), equation (3) reduces to

$$\frac{\partial T^*}{\partial t^*} + v^* \frac{\partial T^*}{\partial y^*} = \alpha \frac{\partial^2 T^*}{\partial y^{*2}} + \frac{16\sigma_s T_\infty^3}{3k_e \rho c_p} \frac{\partial^2 T^*}{\partial y^{*2}} + \frac{v}{c_p} \left(\frac{\partial u^*}{\partial y^*} \right)^2 \tag{8}$$

Introduce the following dimensionless quantities:

$$\left. \begin{aligned} y &= \frac{\bar{u} y^*}{v}, t = \frac{\bar{u}^2 t^*}{v}, u = \frac{u^*}{\bar{u}}, U(t) = \frac{U^*(t^*)}{\bar{u}}, \omega = \frac{\omega^* v}{\bar{u}^2}, \theta = \frac{T^* - T_\infty}{T_w - T_\infty} \\ Gr &= \frac{v g \beta (T_w - T_\infty)}{\bar{u}^3}, Gm = \frac{v g \beta^* (C_w - C_\infty)}{\bar{u}^3}, M = \frac{\sigma \beta_0^2 v}{\rho \bar{u}^2}, R = \frac{k_e k}{4\sigma_s T_\infty^3} \\ C &= \frac{C^* - C_\infty}{C_w - C_\infty}, Pr = \frac{v}{\alpha}, Sc = \frac{v}{D}, Ec = \frac{\bar{u}^2}{c_p (T_w - T_\infty)}. \end{aligned} \right\}$$

Equations (2), (4) and (8) reduce to the following non-dimensional form

$$\frac{\partial u}{\partial t} - \frac{\partial u}{\partial y} = \frac{\partial^2 u}{\partial y^2} - Mu + Gr\theta + GmC \tag{9}$$

$$\frac{\partial \theta}{\partial t} - \frac{\partial \theta}{\partial y} = \frac{1}{Pr} \left(1 + \frac{4}{3R} \right) \frac{\partial^2 \theta}{\partial y^2} + Ec \left(\frac{\partial u}{\partial y} \right)^2 \tag{10}$$

$$\frac{\partial C}{\partial t} - \frac{\partial C}{\partial y} = \frac{1}{Sc} \frac{\partial^2 C}{\partial y^2} \tag{11}$$

The corresponding initial and boundary conditions are as:

$$\left. \begin{aligned} t \leq 0: & u = 0, \theta = 0, C = 0 \\ t > 0: & u = 1, \theta = 1, C = 1 \quad \text{at } y = 0 \\ & u = U(t), \theta = 0, C = 0 \quad \text{at } x = 0 \\ & u \rightarrow U(t), \theta \rightarrow 0, C \rightarrow 0 \quad \text{as } y \rightarrow \infty \end{aligned} \right\} \tag{12}$$

3 Method of solution

Equations (9-11) are coupled non-linear partial differential equations and these can't be solved in closed form. However, these equations can be reduced to a set

of ordinary differential equations and this can be done by representing the velocity, temperature and concentration of the fluid in the neighbourhood of the plate as:

$$\left. \begin{aligned} u(y,t) &= u_0(y) + \varepsilon f(t) u_1(y) \\ \theta(y,t) &= \theta_0(y) + \varepsilon f(t) \theta_1(y) \\ C(y,t) &= C_0(y) + \varepsilon f(t) C_1(y) \\ \text{Also} \\ U(t) &= (1 + \varepsilon f(t)) \end{aligned} \right\} \quad (13)$$

Case (I): We consider a function of time in imaginary form, $f(t) = e^{i\omega t}$.

Substituting the equation (13) into the equations (9-11), we obtain the following equations by considering harmonic and non-harmonic terms while neglecting the higher terms with order of $O(\varepsilon)^2$

$$u_0'' + u_0' - M u_0 = -Gr \theta_0 - G_m C_0 \quad (14)$$

$$\theta_0'' + N_2 \theta_0' = -Ec N_2 \left(\frac{\partial u_0}{\partial y} \right)^2 \quad (15)$$

$$C_0'' + Sc C_0' = 0 \quad (16)$$

subject to the boundary conditions

$$\left. \begin{aligned} u_0 &= 1, \theta_0 = 1, C_0 = 1 \text{ at } y = 0 \\ u_0 &\rightarrow 1, \theta_0 \rightarrow 0, C_0 \rightarrow 0 \text{ as } y \rightarrow \infty \end{aligned} \right\} \quad (17)$$

First-order equations

$$u_1'' + u_1' - N_1 u_1 = -Gr \theta_1 - G_m C_1 \quad (18)$$

$$\theta_1'' + N_2 \theta_1' - N_3 \theta_1 = -2N_2 Ec u_0' u_1' \quad (19)$$

$$C_1'' + Sc C_1' - \omega Sc C_1 = 0 \quad (20)$$

subject to the boundary conditions

$$\left. \begin{aligned} u_1 &= 0, \theta_1 = 0, C_1 = 1 \text{ at } y = 0 \\ u_1 &\rightarrow 1, \theta_1 \rightarrow 0, C_1 \rightarrow 0 \text{ as } y \rightarrow \infty \end{aligned} \right\} \quad (21)$$

To solve the non- linear-coupled equations (14-16) and (18-20), we further assume that the viscous dissipation parameter (Eckert number Ec) is very small for incompressible flows, and therefore, advance an asymptotic expansions for the flow

velocity, temperature and concentration as follows:

$$\left. \begin{aligned} u_0(y) &= u_{01}(y) + Ec u_{02}(y) \\ \theta_0(y) &= \theta_{01}(y) + Ec \theta_{02}(y) \\ C_0(y) &= C_{01}(y) + Ec C_{02}(y) \\ u_1(y) &= u_{11}(y) + Ec u_{12}(y) \\ \theta_1(y) &= \theta_{11}(y) + Ec \theta_{12}(y) \\ C_1(y) &= C_{11}(y) + Ec C_{12}(y) \end{aligned} \right\} \quad (22)$$

Substituting the equation (22) into the equations (14-16) and (18-20), we obtain the following sequence of approximations:

The zeroth order equations are:

$$u_{01}'' + u_{01}' - M u_{01} = -Gr \theta_{01} - Gm C_{01} \quad (23)$$

$$u_{02}'' + u_{02}' - M u_{02} = -Gr \theta_{02} - Gm C_{02} \quad (24)$$

$$\theta_{01}'' + N_2 \theta_{01}' = 0 \quad (25)$$

$$\theta_{02}'' + N_2 \theta_{02}' = -N_2 \left(\frac{\partial u_{01}}{\partial y} \right)^2 \quad (26)$$

$$C_{01}'' + Sc C_{01}' = 0 \quad (27)$$

$$C_{02}'' + Sc C_{02}' = 0 \quad (28)$$

subject to the boundary conditions:

$$\left. \begin{aligned} u_{01} = 1, u_{02} = 0, \theta_{01} = 1, \theta_{02} = 0, C_{01} = 1, C_{02} = 0 \text{ at } y = 0 \\ u_{01} \rightarrow 1, u_{02} \rightarrow 0, \theta_{01} \rightarrow 0, \theta_{02} \rightarrow 0, C_{01} \rightarrow 0, C_{02} \rightarrow 0 \text{ as } y \rightarrow \infty \end{aligned} \right\} \quad (29)$$

The first - order equations are:

$$u_{11}'' + u_{11}' - N_1 u_{11} = -Gr \theta_{11} - Gm C_{11} \quad (30)$$

$$u_{12}'' + u_{12}' - N_1 u_{12} = -Gr \theta_{12} - Gm C_{12} \quad (31)$$

$$\theta_{11}'' + N_2 \theta_{11}' - N_3 \theta_{11} = 0 \quad (32)$$

$$\theta_{12}'' + N_2 \theta_{12}' - N_3 \theta_{12} = -2N_2 u_{01}' u_{11}' \quad (33)$$

$$C_{11}'' + Sc C_{11}' - \omega Sc C_{11} = 0 \quad (34)$$

$$C_{12}'' + Sc C_{12}' - \omega Sc C_{12} = 0 \quad (35)$$

where

$$N_1 = M + i\omega, N_2 = \frac{3RPr \omega}{3R + 4}, N_3 = \frac{3iRPr \omega}{3R + 4}$$

Subject to the boundary conditions:

$$\left. \begin{aligned} u_{11} = 0, u_{12} = 0, \theta_{11} = 0, \theta_{12} = 0, C_{11} = 0, C_{12} = 0 \text{ at } y = 0 \\ u_{11} \rightarrow 1, u_{12} \rightarrow 0, \theta_{11} \rightarrow 0, \theta_{12} \rightarrow 0, C_{11} \rightarrow 0, C_{12} \rightarrow 0 \text{ as } y \rightarrow \infty \end{aligned} \right\} \quad (36)$$

Equations (23 -28) are solved with the boundary conditions (29) and equations (30-35) are solved with the boundary conditions (36), we get velocity, temperature and concentration as:

$$\begin{aligned} u(y,t) = & ((\alpha_1 + \alpha_2)e^{-m_1y} + 1 - \alpha_1e^{-N_2y} - \alpha_2e^{-Scy}) + Ec(\alpha_{17}e^{-m_1y} \\ & - \alpha_{10}e^{-N_2y} - \alpha_{11}e^{-2m_1y} - \alpha_{12}e^{-2N_2y} - \alpha_{13}e^{-2Scy} + \alpha_{14}e^{-[m_1+N_2]y} \\ & + \alpha_{15}e^{-[m_1+Sc]y} - \alpha_{16}e^{-[N_2+Sc]y}) + \varepsilon e^{i\omega t} ((1 - e^{-m_2y}) \\ & + Ec(\alpha_{26}e^{-m_1y} - \alpha_{22}e^{-m_3y} - \alpha_{23}e^{-[m_1+m_2]y} + \alpha_{24}e^{-[N_2+m_2]y} \\ & + \alpha_{25}e^{-[Sc+m_2]y})). \end{aligned} \quad (37)$$

$$\begin{aligned} \theta(y,t) = & (e^{-N_2y} + Ec(\alpha_9e^{-N_2y} + \alpha_3e^{-2m_1y} + \alpha_4e^{-2N_2y} + \alpha_5e^{-2Scy} \\ & - \alpha_6e^{-[m_1+N_2]y} - \alpha_7e^{-[m_1+Sc]y} + \alpha_8e^{-[Sc+N_2]y})) \\ & + \varepsilon e^{i\omega t} Ec(\alpha_{21}e^{-m_3y} + \alpha_{18}e^{-[m_1+m_2]y} - \alpha_{19}e^{-[N_2+m_2]y} \\ & - \alpha_{20}e^{-[Sc+m_2]y}). \end{aligned} \quad (38)$$

$$C(y,t) = e^{-Scy}. \quad (39)$$

Case (II): Now we consider a function of time in real form, $f(t) = e^{\omega t}$.

By following the same procedure as in case I, we draw the graphs for velocity and temperature profiles in this case.

4 Result and Discussion

Here, we have formulated and solved the problem of the MHD free convection of a radiating electrically conducting fluid over a cooling ($Gr > 0$) vertical plate by making fairly realistic asymptotic approximation and we depict the comparison of the results of two particular cases. In numerical computation, the Prandtl number ($Pr = 0.7$) corresponding to air and other values of the material parameters are used. In addition, the boundary condition $y \rightarrow \infty$ is approximated by $y_{max} = 30$ and $y_{max} = 18$, which is sufficiently large for the velocity and temperature, respectively to approach their free stream values. In the subsequent analysis, we started with temperature profiles due to its primary importance in astrophysical environments. The temperature profiles are presented when the free convection currents are cooling the plate.

4.1 Effects of frequency of excitation over temperature profiles

The effect of frequency of excitation on the temperature profiles has been illustrated in figures 1(a) and 1(b). From figure 1(a), it is clear that as we move far away from the plate, initially the temperature increases rapidly and thereafter decreases rapidly, whereas, in figure 1(b), the frequency of excitation has insignificant effect over thermal boundary layer thickness i.e. the profiles are in very closer range.

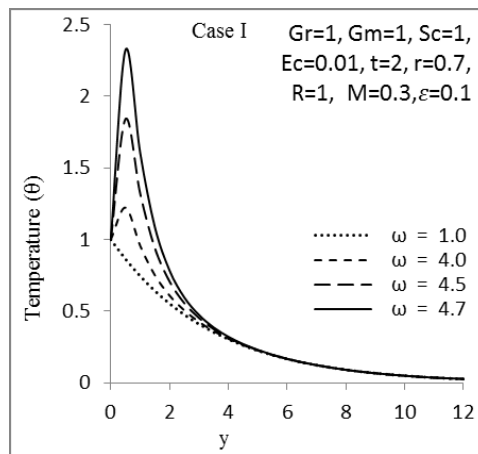


Figure 1(a): Effect of frequency of excitation on temperature field.

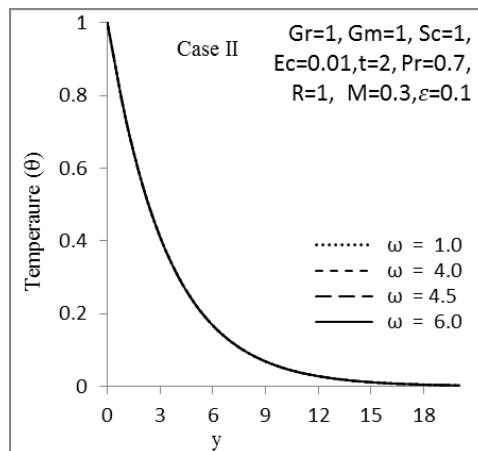


Figure 1(b): Effect of frequency of excitation on temperature field.

4.2 Effects of magnetic intensity over temperature profiles

The effect of magnetic intensity on the temperature profiles is shown through figures 2(a) and 2(b) and all other participating parameters in the temperature field are held constant. From both figures, the effect of magnetic field is found to have zero effect on the temperature throughout the thermal boundary layer thicknesses.

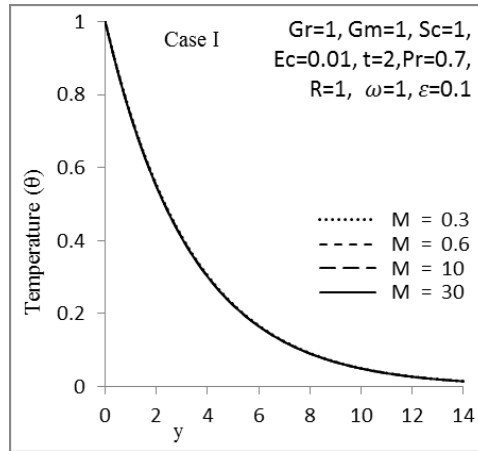


Figure 2(a): Effect of magnetic intensity on temperature field.

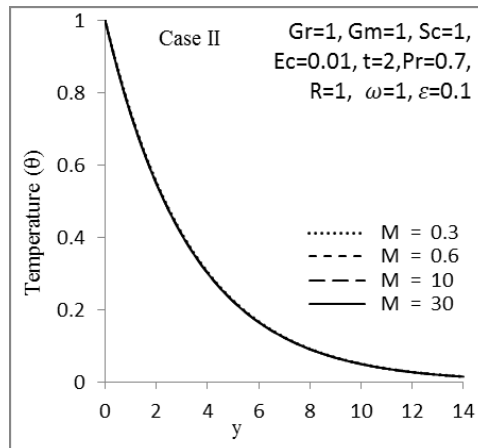


Figure 2(b): Effect of magnetic intensity on temperature field.

4.3 Effects of Prandtl number over temperature profiles

Figures 3(a) and 3(b) exhibit the effect of Prandtl number on temperature profiles. Prandtl number defines the ratio of momentum diffusivity to thermal diffusivity i.e. it controls the thickness of the thermal boundary layer and the rate of heat transfer. For $Pr = 1$, the momentum and thermal boundary thicknesses, as described Schlichting (1979), are approximately of equal extent. We, therefore, expect that with an increase in Pr , the thermal boundary layer will be decreased in thickness and there will be a corresponding uniformity of temperature distributions across the boundary layer. The profiles in both figures attest that the maximum temperature occurs corresponding to lowest Prandtl number, $Pr = 0.1$ (say).

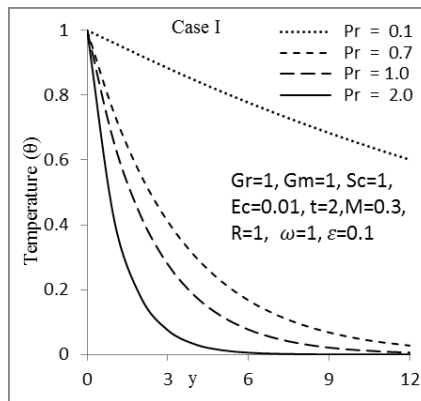


Figure 3(a): Effect of Prandtl number on temperature field.

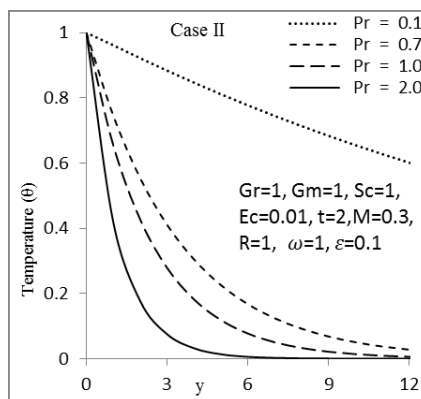


Figure 3(b): Effect of Prandtl number on temperature field.

4.4 Effects of radiation parameter over temperature profiles

We observe from figures 4(a) and 4(b) that an increase in the conduction-radiation parameter (R i.e Stark number) is associated with a decrease in temperature. An increase in R corresponds to an increase in the relative contribution of conduction heat transfer to thermal radiation heat transfer. As $R \rightarrow \infty$, heat transfer dominates and the contribution of thermal radiative flux vanishes. The converse is true for ($R = 0$) where thermal radiation dominates over conduction, Cookey (2003). Small values of R therefore, physically correspond to stronger thermal radiation flux and accordingly, the maximum temperatures are observed in both cases for $R = 0.1$. As R increases to 0.4, 1 and 2, considerable reduction is observed in the temperature values θ from the peak value at the wall $y = 0$, across the boundary layer regime to the free stream at $y = 30$ and for onward values of $R (> 2)$, the temperature variations are negligible.

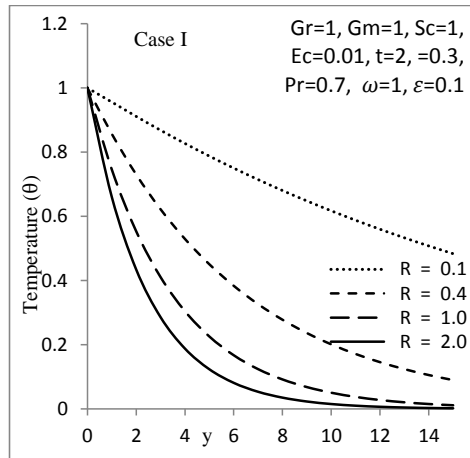


Figure 4(a): Effect of radiation parameter on temperature field.

4.5 Effects of Schmidt number over temperature profiles

Figures 5(a) and 5(b) clearly indicate that Schmidt number does not have a noticeable change in temperature field i.e the profiles are in very closer range. A rise in Schmidt number from 0.1, 0.5, 1 and 10 all through induces a fall in temperature, where values of $Sc = 0.3, 0.5, 0.6, 0.78$ and 1 approximately represent helium, water, water vapor, ammonia and Carbon Dioxide, respectively. Higher values of Schmidt number are associated with hydrocarbon working fluids like ($Sc = 2$) for Ethyl Benzene.

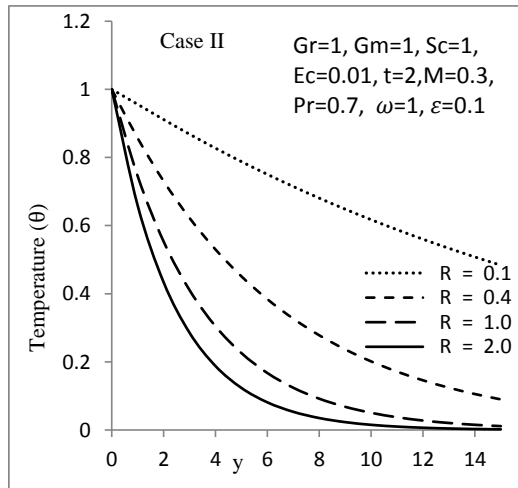


Figure 4(b): Effect of radiation parameter on temperature field.

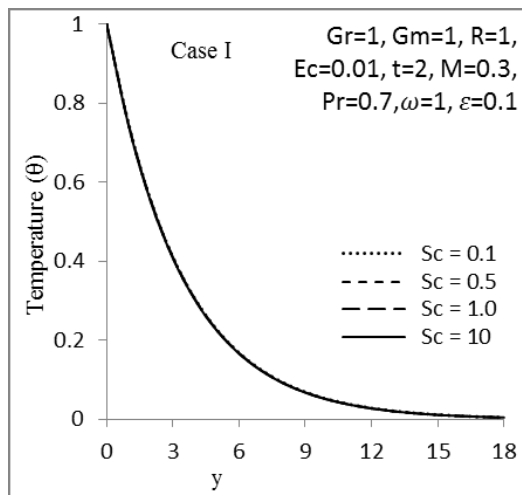


Figure 5(a): Effect of Schmidt number on temperature field.

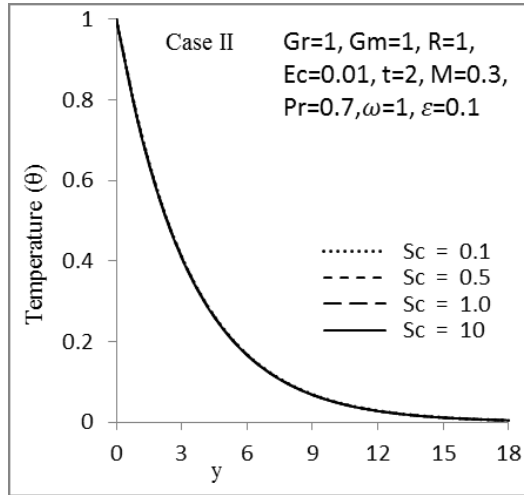


Figure 5(b): Effect of Schmidt number on temperature field.

4.6 Effects of Grashof number over temperature profiles

Figures 6(a) and 6(b) represent the temperature field for different values of Grashof number. The results show that increased cooling ($Gr > 0$) of the plate leads to a rise in the temperature field in both cases. As we move away from the plate, we notice that, a smaller value of Grashof number does not contribute much on the temperature field but a higher value contributes to the increase in the temperature. A similar trend is observed for the solutal Grashof number, as shown in figures 7(a) and 7(b). Again temperatures are seen to rise with a rise in solutal Grashof number from 1 to 50, but in these figures, the peak values are 1.1590227 and 1.1405984, respectively, corresponding to $Gm = 50$ at displacement $y = 1$.

4.7 Effects of Eckert number over temperature profiles

The variation in the temperature profiles with respect to viscous dissipation parameter is illustrated in figures 8(a) and 8(b). These graphs have the same trend as described in figures 6(a) and 6(b), however, they have different peak values such as 1.6813321 and 1.2217963, respectively, corresponding to $Ec = 1.2$ at displacement $y = 1$.

4.8 Effects of magnetic intensity over velocity

Figures 9(a) and 9(b) represent the dimensionless velocity profiles for different values of magnetic intensity. Smaller values of magnetic field have much effect over

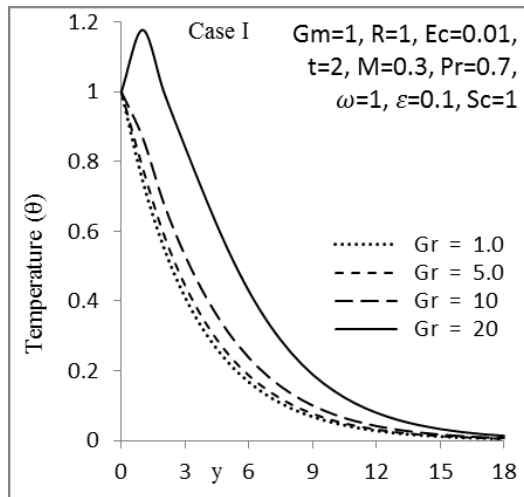


Figure 6(a): Effect of free convection parameter on temperature field.

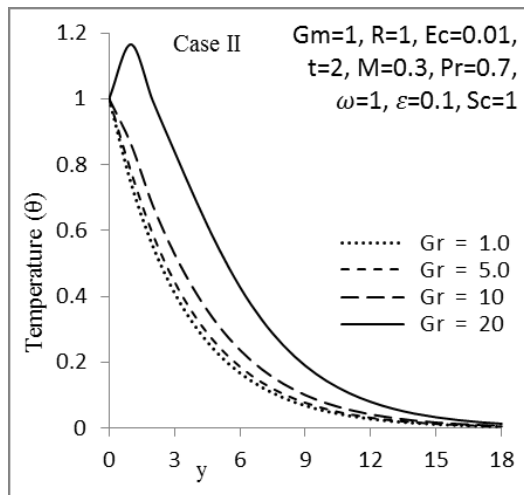


Figure 6(b): Effect of free convection parameter on temperature field.

velocity profiles. For sufficiently higher values, the relation between the magnetic parameter and velocity profiles is properly linear. In both figures, it is noticed that as magnetic parameter increases the velocity profile decreases.

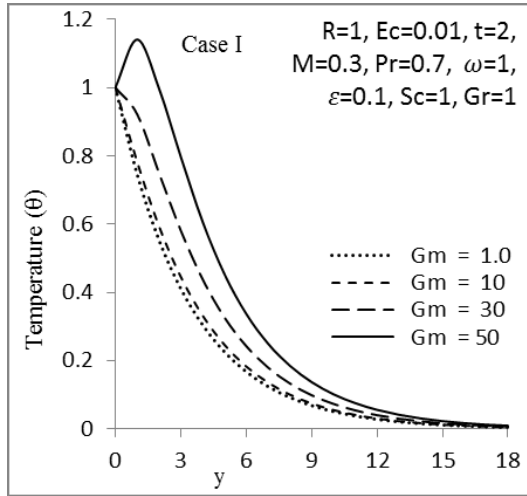


Figure 7(a): Effect of solutal Grashof number on temperature field.

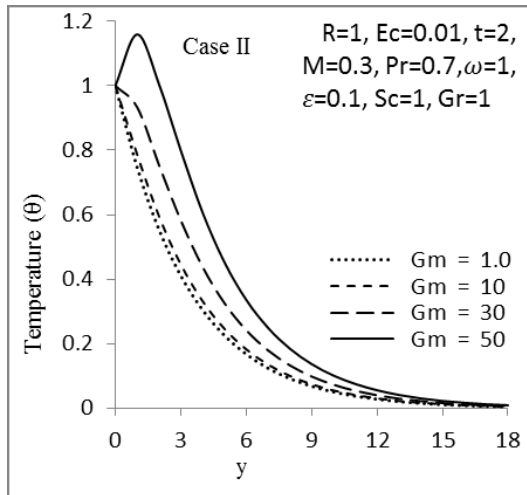


Figure 7(b): Effect of solutal Grashof number on temperature field.

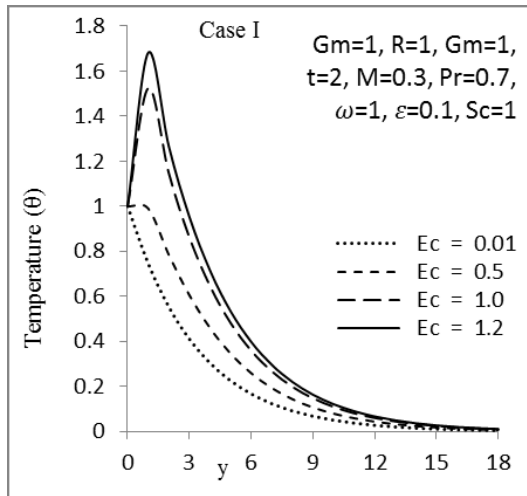


Figure 8(a): Effect of Eckert number on temperature field.

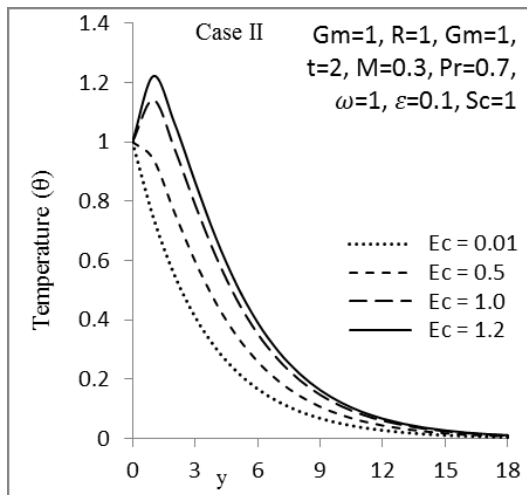


Figure 8(b): Effect of Eckert number on temperature field.

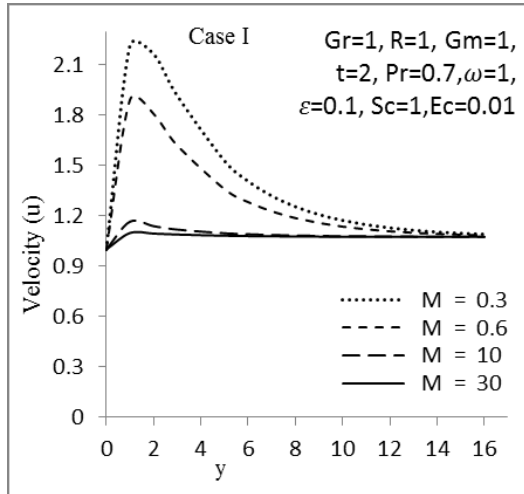


Figure 9(a): Effect of magnetic intensity on velocity field.

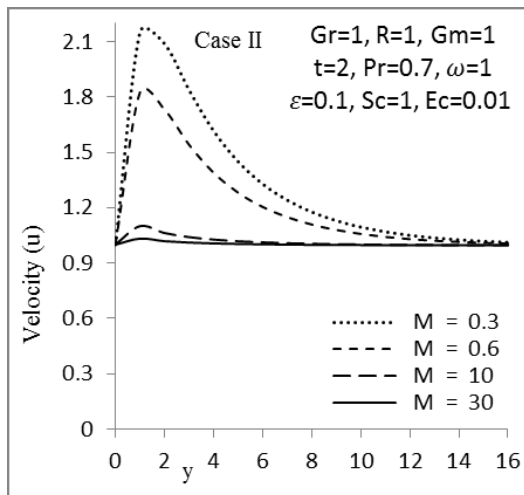


Figure 9(b): Effect of magnetic intensity on velocity field.

4.9 Effects of Prandtl number, radiation parameter and Schmidt number over velocity profiles

Figures (10-12) display the effect of Prandtl number radiation parameter and Schmidt number over velocity profiles, respectively. These graphs have the same trend i.e. the velocity field is decreasing for increasing values of Pr , R and Sc . It is evident from all these graphs that velocity profiles remain the same after displacement $y = 260$ onwards at its free stream values approximate to 1.0738906.

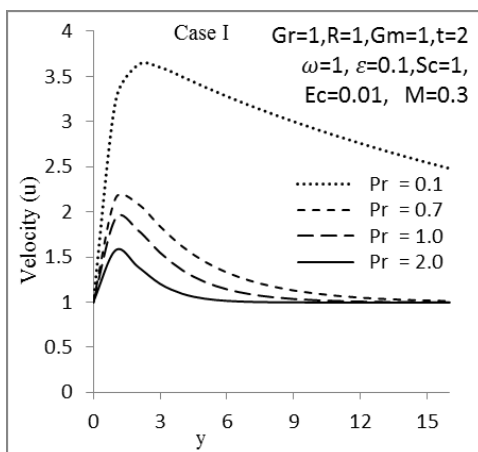


Figure 10(a): Effect of Prandtl number on velocity field.

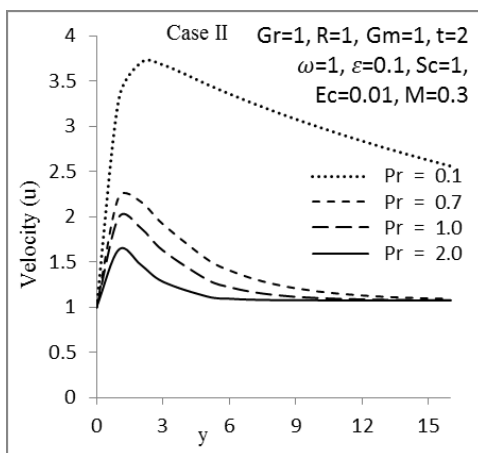


Figure 10(b): Effect of Prandtl number on velocity field.

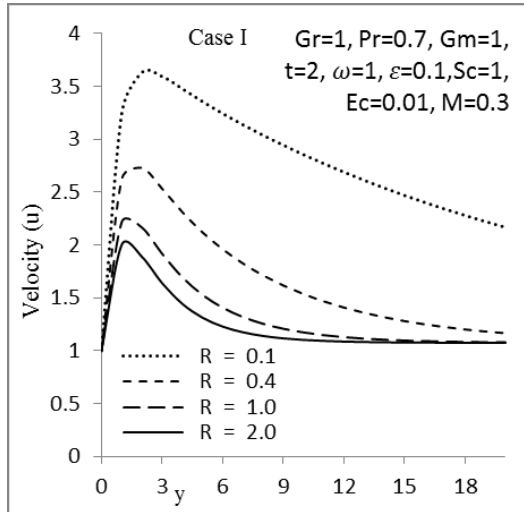


Figure 11(a): Effect of radiation parameter on velocity field.

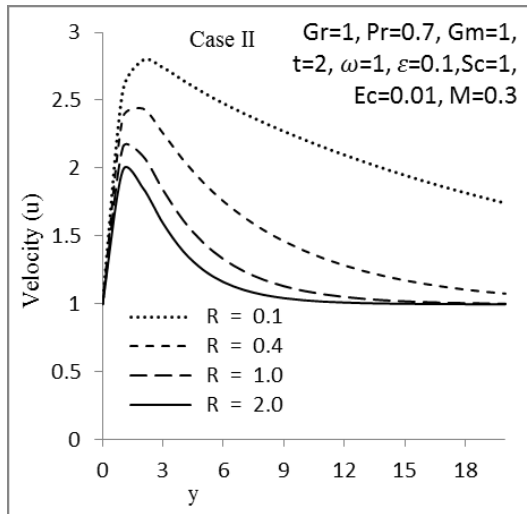


Figure 11(b): Effect of radiation parameter on velocity field.

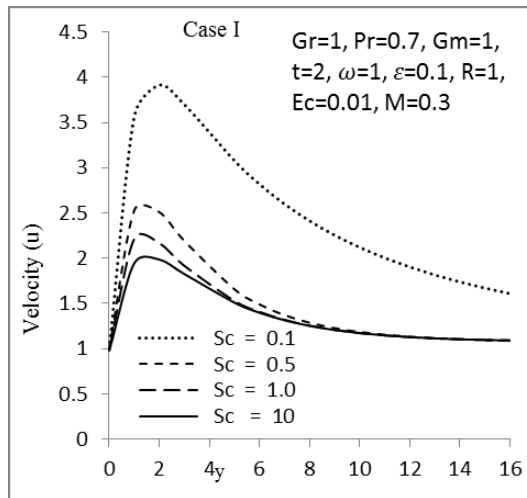


Figure 12(a): Effect of Schmidt number on velocity field.

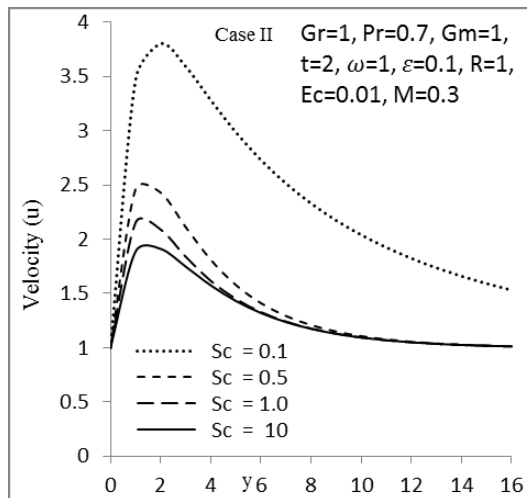


Figure 12(b): Effect of Schmidt number on velocity field.

4.10 Effects of Grashof number, solutal Grashof number and Eckert number over velocity profiles

Figures (13-15) illustrate the influence of the thermal buoyancy effects, concentration buoyancy effects and viscous dissipation parameter over velocity profiles, respectively. In these graphs, the velocity distribution attains a distinctive maximum value in the vicinity of the plate surface and then decreases properly to approach the free stream value. As expected, the fluid velocity increases and the peak value becomes more distinctive for increasing values of Grashof number, solutal Grashof number and Eckert number.

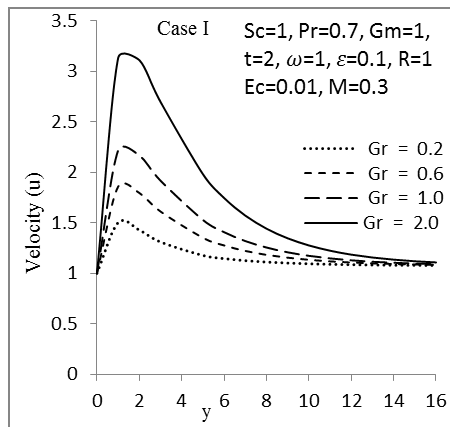


Figure 13(a): Effect of free convection parameter on velocity field.

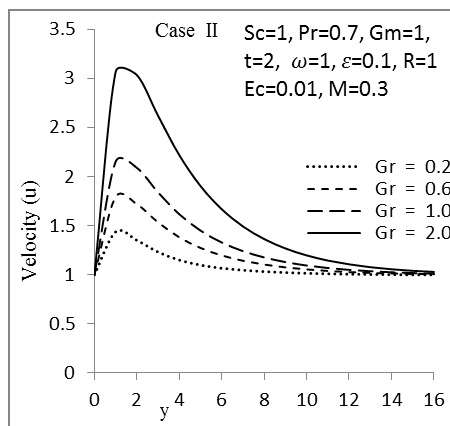


Figure 13(b): Effect of free convection parameter on velocity field.

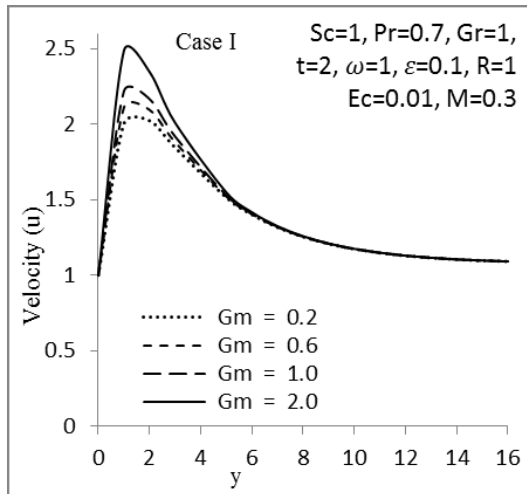


Figure 14(a): Effect of solutal Grashof number on velocity field.

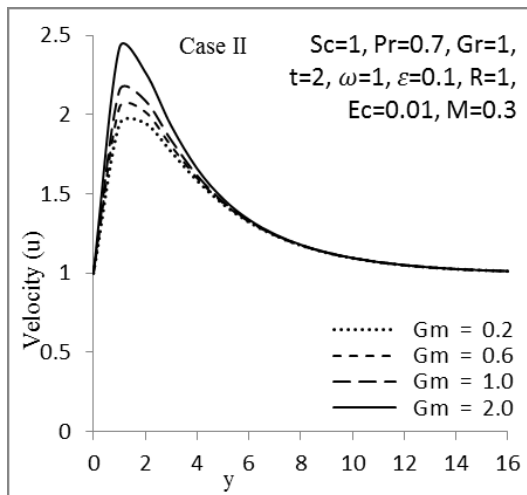


Figure 14(b): Effect of solutal Grashof number on velocity field.

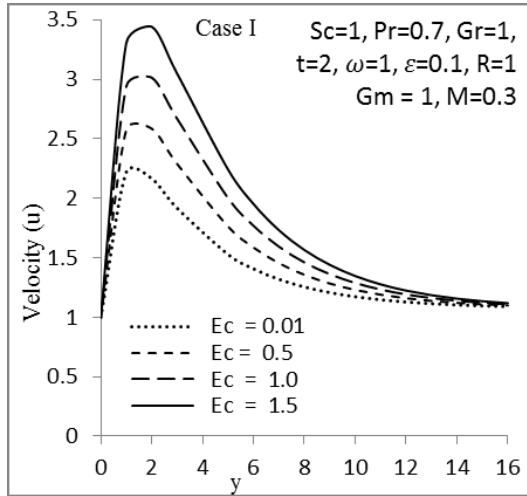


Figure 15(a): Effect of Eckert number on velocity field.

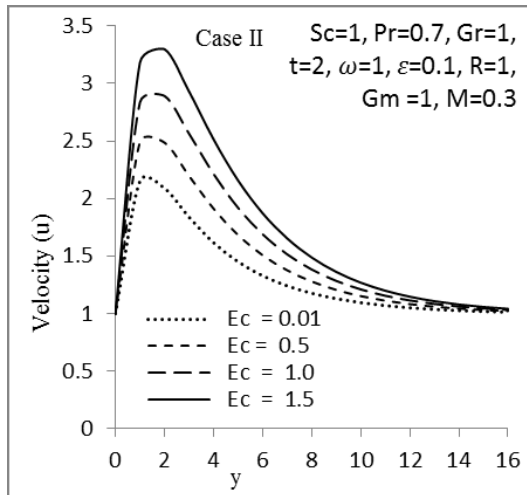


Figure 15(b): Effect of Eckert number on velocity field.

4.11 Effects of frequency of excitation over velocity profiles

Figures 16(a) and 16(b) depict the effects of frequency of excitation versus y on velocity profiles, for constant values of other parameters. It is noticed that as the frequency of excitation increases, the velocity field decreases. Further, it is observed that as we move far away from the plate, the velocity increases rapidly initially and thereafter, the decrease is found to be slow. However, this parameter has insignificant effect over velocity profiles i.e. the profiles are in very closer range as shown in figure 16(b), whereas, in figure 16(a) it shows relatively more effect on velocity profiles.

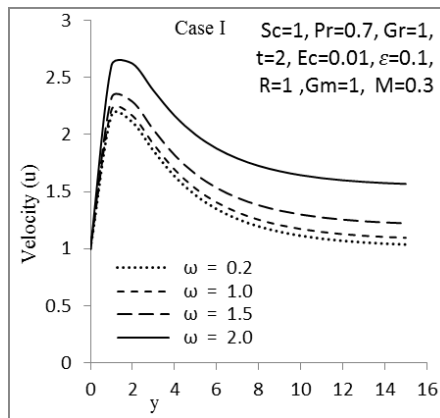


Figure 16(a): Effect of frequency of excitation on velocity field.

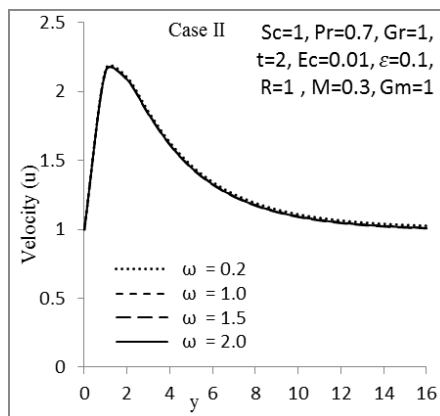


Figure 16(b): Effect of frequency of excitation on velocity field.

5 Concluding remarks

The governing equations for a problem of unsteady MHD free convection (producing a fluctuating flow past an impulsively started isothermal vertical plate with radiation and viscous dissipation) were formulated and solved. Such a study has background applications in geophysical flows and in certain industrial situations.

The plate velocity was maintained at a constant value and the flow was subjected to a transverse magnetic field. It was found in brief.

- Increasing the values of Pr and R reduces the temperature and velocity, whereas a rise in Gr , Gm and Ec increases the temperature and velocity along the wall and along the direction transverse to the wall.
- Schmidt number and Hartman number do not have much effect on temperature profiles.
- A rise in M and Sc induces a substantial fall in velocity.
- In figures 1(b) and 16(b), frequency of excitation does not have much effect over temperature and velocity profiles, respectively.
- Whereas in figures 1(a) and 16(a), a rise in frequency of excitation increases the temperature and velocity profiles along the wall and transverse to the wall and the transverse direction.

References

Abd EI-Naby, M. A.; Elbarbary Elsayed, M. E.; Abdelazem Nader, Y.; (2003): Finite difference solution of radiation effects on MHD free convection flow over a vertical plate with variable surface temperature. *J. Appl. Mathematics*, vol. 2, no. 2, pp. 65-86.

Brewster, M.Q. (1992): *Thermal Radiative Transfer and Properties*. John Wiley & Sons. Inc., New York.

Chamkha, A. J.; Takhar, H. S.; Soundalgekar, V. M. (2001): Radiation effects on free convection flow past a semi-infinite vertical plate with mass transfer. *Chemical Engineering J.*, vol. 84, no. 3, pp. 335-342.

Das, U. N.; Deka, R.; Soundalgekar, V. M. (1994): Effects of mass transfer on flow past an impulsively started infinite vertical plate with constant heat flux and chemical reaction. *Forschung Im Ingenieurwesen*, vol. 60, no. 10, pp. 284-287.

Israel-Cookey, C.; Ogulu, A.; Omubo-Pepple, V.B. (2003): Influence of viscous dissipation and radiation on unsteady MHD free convection flow past an infinite

heated vertical plate in porous medium with time dependent suction. *Int. J. Heat Mass Transfer*, vol. 46, no. 13, pp. 2305-2311.

Israel-Cookey, C.; Nwaigwe, C. (2010): Unsteady MHD flow of a radiating fluid over a moving heated porous plate with time dependent suction. *American J. of Sci. Ind. Res.*, vol. 1, no. 1, pp. 88-95.

Ibrahim, F. S.; Elaiw, A. M.; Bakr, A. A. (2008): Effect of the chemical reaction and radiation absorption on the unsteady MHD free convection flow past a semi-infinite vertical permeable moving plate with heat source and suction. *Comm. Non-linear Sci. Numer Simulat.*, vol. 13, pp. 1056-1066.

Loganathan, P.; Ganesan, P. (2006): Effects of radiation on flow past an impulsively started infinite vertical plate with mass transfer. *J. Engineering Physics and Thermophysics*, vol. 79, no. 1, pp. 65-72.

Muthucumaraswamy, R.; Ganesan, P. (1998): Flow past an impulsively started vertical plate with variable surface temperature and mass flux. *Heat and Mass Transfer*, vol. 34, no. 6, pp. 487-493.

Muthucumaraswamy, R. (2004): Natural convection on flow past an impulsively started vertical plate with variable surface heat flux. *Far East J. Applied Mathematics*, vol. 14, no. 1, pp. 99-109.

Makinde, O. D. (2005): Free convection flow with thermal radiation and mass transfer past a moving vertical plate. *Int. Comm. Heat Mass Transfer*, vol. 32, pp. 1411-1419.

Ramachandra Prasad, V.; Bhaskar Reddy, N.; Muthukumaraswamy, R. (2007): Radiation and mass transfer effects on two dimensional flow past an impulsively started infinite vertical plate. *Int. J. Thermal Sciences*, vol. 46, no. 12, pp. 1251-1258.

Rapits, A.; Perdikis, C. (1999): The effects of thermal radiation on free convective flow past a moving vertical plate. *Int. J. Appl. Mech. and Engineering*, vol. 8, pp. 125.

Ram, P.; Kumar, A.; Singh, H. (2013): Effect of porosity on unsteady MHD flow past a semi-infinite moving vertical plate with time dependent suction. *Indian J. Pure and Appl. Phys.*, vol. 51, no. 7, pp. 461-470.

Ramana Murthy, C. V.; Prasad, P. H. (2011): Flow past a semi-infinite moving vertical plate with viscous dissipation under the influence of magnetic field. *Advances in Theoretical and Appl. Math.*, vol. 6, no. 1, pp. 73-87.

Ramana Murthy, C. V.; Madana Mohana Rao, A.; Ramana Reddy, G. V. (2010): Effects of radiation and mass transfer on MHD free convection flow past an impulsively started isothermal vertical plate with viscous dissipation. *J. Comp.*

and *Math. Science*, vol. 1, no. 5, pp. 538-551.

Schlichting, H. (1979): *Boundary-Layer Theory*, 7th edition, Mac Graw-Hill.

Suneetha, S.; Bhaskar Reddy, N.; Ramachandra Prasad, V. (2011): Radiation and mass transfer effects on MHD free convective dissipative fluid in the presence of heat source/ sink. *J. Appl. Fluid Mech.*, vol. 4, no.1, pp. 107-113.

Takhar, H.S.; Beg, O.A.; Chamkha, A.J.; Filip, D.; Pop, I. (2003): Mixed radiation-convection boundary layer flow of an optically dense fluid along a vertical flat plate in a non-darcy porous medium. *Int. J. Appl. Mech. and Engg.*, vol. 8, pp. 483-496.

Appendix

$$m_1 = 0.5[1 + \sqrt{(1 + 4M)}]$$

$$m_2 = 0.5[1 + \sqrt{(1 + 4N_1)}]$$

$$m_3 = 0.5[N_2 + \sqrt{(N_2^2 + 4N_3)}]$$

$$\alpha_1 = Gr / (N_2^2 - N_2 - M)$$

$$\alpha_2 = Gm / (Sc_2^2 - Sc - M)$$

$$\alpha_3 = \frac{N_2 m_1^2 (\alpha_1 + \alpha_2)^2}{4m_1^2 - 2m_1 N_2}$$

$$\alpha_4 = \frac{\alpha_1^2 N_2^3}{2N_2^2}$$

$$\alpha_5 = \frac{\alpha_2^2 N_2 Sc^2}{4Sc^2 - 2N_2 Sc}$$

$$\alpha_6 = \frac{2m_1 N_2^2 (\alpha_1 + \alpha_2) \alpha_1}{(m_1 + N_2)^2 - N_2 (m_1 + N_2)}$$

$$\alpha_7 = \frac{2m_1 N_2 Sc (\alpha_1 + \alpha_2) \alpha_2}{(m_1 + Sc)^2 - N_2 (m_1 + Sc)}$$

$$\alpha_8 = \frac{2\alpha_1 \alpha_2 N_2^2 Sc}{(N_2 + Sc)^2 - N_2 (N_2 + Sc)}$$

$$\alpha_9 = -(\alpha_3 - \alpha_4 - \alpha_5 + \alpha_6 + \alpha_7 - \alpha_8)$$

$$\alpha_{10} = \frac{Gr \alpha_9}{N_2^2 - N_2 - M}$$

$$\alpha_{11} = \frac{Gr \alpha_3}{4m_1^2 - 2m_1 - M}$$

$$\alpha_{12} = \frac{Gr \alpha_4}{4N_2^2 - 2N_2 - M}$$

$$\alpha_{13} = \frac{Gr \alpha_5}{4Sc^2 - 2Sc - M}$$

$$\alpha_{14} = \frac{Gr \alpha_6}{(m_1 + N_2)^2 - (m_1 + N_2) - M}$$

$$\alpha_{15} = \frac{Gr \alpha_7}{(m_1 + Sc)^2 - (m_1 + Sc) - M}$$

$$\alpha_{16} = \frac{Gr \alpha_8}{(N_2 + Sc)^2 - (N_2 + Sc) - M}$$

$$\alpha_{17} = (\alpha_{10} + \alpha_{11} + \alpha_{12} + \alpha_{13} - \alpha_{14} - \alpha_{15} + \alpha_{16})$$

$$\alpha_{18} = \frac{2m_1 m_2 N_2 (\alpha_1 + \alpha_2)}{(m_1 + m_2)^2 - N_2(m_1 + m_2) - N_3}$$

$$\alpha_{19} = \frac{2\alpha_1 m_2 N_2^2}{(N_2 + m_2)^2 - N_2(N_2 + m_2) - N_3}$$

$$\alpha_{20} = \frac{2\alpha_2 N_2 Sc}{(Sc + m_2)^2 - N_2(Sc + m_2) - N_3}$$

$$\alpha_{21} = -(\alpha_{18} - \alpha_{19} - \alpha_{20})$$

$$\alpha_{22} = \frac{Gr \alpha_{21}}{m_3^2 - m_3 - N_1}$$

$$\alpha_{23} = \frac{Gr \alpha_{18}}{(m_1 + m_2)^2 - (m_1 + m_2) - N_1}$$

$$\alpha_{24} = \frac{Gr \alpha_{19}}{(N_2 + m_2)^2 - (N_2 + m_2) - N_1}$$

$$\alpha_{25} = \frac{Gr \alpha_{20}}{(Sc + m_2)^2 - (Sc + m_2) - N_1}$$

$$\alpha_{26} = (\alpha_{22} + \alpha_{23} - \alpha_{24} - \alpha_{25})$$